Topographical Quantification of Retinal Fluid in Type 3 MNV and Associations With Short-Term Visual Outcomes

ALESSANDRO BERNI, JONATHAN D. OAKLEY, ROSA DOLZ-MARCO, ROBERTO GALLEGO-PINAZO, FRANCESCA CIMOROSI, ANDREA GHILARDI, DANIEL B. RUSSAKOFF, COSTANZA BARRESI, UGO INTROINI, MICHELE REIBALDI, FRANCESCO BANDELLO, AND ENRICO BORRELLI

• PURPOSE: This study aims to quantify the volume of intraretinal fluid (IRF), subretinal fluid (SRF), and subretinal pigment epithelium (sub-RPE) fluid in treatment-naïve Type 3 macular neovascularization (MNV) eyes with age-related macular degeneration (AMD) and to investigate the correlation of these fluid volumes with visual acuity (VA) outcomes at baseline and following antivascular endothelial growth factor (VEGF) treatment.

• DESIGN: Retrospective, clinical cohort study.

• METHODS: In this study, we analyzed patients diagnosed with exudative AMD and treatment-naïve Type 3 MNV undergoing a loading dose of anti-VEGF therapy. Using a validated deep-learning segmentation strategy, we processed optical coherence tomography (OCT) B-scans to segment and quantify IRF (i.e., both in the inner and outer retina), SRF, and sub-RPE fluid volumes at baseline. The study correlated baseline fluid volumes with baseline and short-term VA outcomes postloading dose of anti-VEGF injections.

• RESULTS: Forty-six eyes from 46 patients were included in this study. Visual acuity was 0.51 ± 0.30 LogMAR at baseline and 0.33 ± 0.20 LogMAR after the loading dose of anti-VEGF ($P = .001$). Visual acuity at the follow-up visit was 0.40 ± 0.17 LogMAR in patients with no complete resolution of retinal fluid and 0.31 ± 0.20 LogMAR in eyes without retinal fluid after treatment ($P = .225$). In the multivariable analysis, the IRF volume in the inner retina ($P = .032$) and the distance of the MNV from the fovea ($P = .037$) were predictors of visual acuity at baseline. The baseline IRF volume in the inner retina also predicted the visual acuity at follow-up ($P = .023$).

• CONCLUSION: The present study highlights the fluid volume in the inner retina as a crucial predictor of short-term visual outcomes in Type 3 MNV, underscoring the detrimental effect of IRF on neuroretinal structures. (Am J Ophthalmol 2025;269: 181–188. © 2025 The Authors. Published by Elsevier Inc. This is an open access article under the CC BY license (http://creativecommons.org/licenses/by/4.0/))

INTRODUCTION

TYPE 3 MACULAR NEOVASCULARIZATION (MNV), ALSO known as retinal angiomatous proliferation (RAP), represents a distinct subtype of neovascularization primarily associated with age-related macular degeneration (AMD).[1-3] This form is distinctive because it originates within the deep retinal capillary plexus, diverging from the choroidal origin seen in Type 1 and Type 2 MNVs.[2,4,5] Type 3 MNV is responsible for approximately 30%-40% of all new cases of neovascular AMD (nAMD),[6] underscoring its clinical importance.

Patients with Type 3 MNV typically show a positive initial response to antivascular endothelial growth factor (anti-VEGF) therapy, demonstrating significant fluid resolution.[7-11] Nonetheless, this does not always translate to optimal visual outcomes, mostly due to the development of macular atrophy, a complication frequently found in eyes with Type 3 MNV.[8,12-14] This atrophy may result from direct mechanical damage by neovascular formations to the retinal pigment epithelium (RPE), from the collapse of serous pigment epithelial detachment (PED) associated with the MNV, or from the development of fibrosis.[15] Additionally, atrophy may stem from factors independent of MNV, such as drusen or subretinal drusenoid deposits (SDDs).[15]

Interestingly, reduced visual acuity (VA) has been reported even in cases without apparent outer retinal atrophy, hinting at additional contributory factors to central vision loss.[16] According to Su et al.,[9] an optical coherence tomography (OCT) classification for active Type 3 MNVs includes the presence of intraretinal fluid (IRF) across all

AJO.com Supplemental Material available at AJO.com.

Accepted for publication August 22, 2024.

The IRCCS San Raffaele Scientific Institute (A.B., C.B., U.I., F.B.), Milan, Italy; Vita-Salute San Raffaele University Milan (A.B., C.B., U.I., F.B.), Milan, Italy; Voxeleron Inc. (J.D.O., D.B.R.), Austin, Texas, United States; Unit of Macula, Oftalvist Clinic (R.D.-M., R.G.-P.), Valencia, Spain; Department of Surgical Sciences, University of Turin (F.C., A.G., M.R., E.B.), Turin, Italy; Department of Ophthalmology, City of Health and Science Hospital (F.C., A.G., M.R., E.B.), Turin, Italy

Inquiries to Enrico Borrelli, MD, PhD, FEBO, Department of Ophthalmology, University of Turin, Via Cherasco, 23, Turin, Italy; e-mail: borrelli.enrico@yahoo.com

0002-9394/$36.00
https://doi.org/10.1016/j.ajo.2024.08.024

stages, making it a defining characteristic of Type 3 MNVs. While early stages are typically marked by small intraretinal cysts (stage 1), Type 3 MNVs usually progress toward the RPE causing its disruption and PED formation (stage 2). This latter facilitates neovascular proliferation beneath the RPE, resulting in sub-RPE fluid accumulation and serous PEDs development (stage 3). Such PEDs eventually lead to subretinal fluid (SRF) accumulation around their edges when larger fluid volumes shift into subretinal and sub-RPE spaces following outer retinal collapse at the lesion site. Since SRF and sub-RPE fluid are present in the later stage of Type 3 progression, they are thought to be commonly associated with significant IRF volumes.

Extending Su et al.'s classification, Sharma and collaborators[17] explored all the associations among the three fluid types characterizing Type 3 MNVs: IRF, SRF, and sub-RPE fluid. Their findings indicate that patients presenting with isolated IRF (stages 1 and 2) generally exhibit a more favorable visual prognosis than those where IRF coexists with SRF and/or sub-RPE fluid (stage 3). This led them to propose that the presence of SRF and sub-RPE fluid might determine more extensive retinal damage, thereby contributing to greater visual impairment. While the collapse of serous PEDs could be associated with atrophy formation and visual loss, the specific impact of SRF remains controversial. Haj Najeeb et al.[18] observed that SRF, typically located at the periphery of PEDs, seldom impacts the fovea directly, suggesting its limited effect on VA. Conversely, the significant volume of IRF present in eyes with SRF could impair visual outcomes by damaging intraretinal cells and, therefore, be the determinant of visual loss in these patients.

The consistent presence of IRF throughout all Type 3 MNV stages indicates that its potential as a prognostic factor cannot be solely based on its presence. Instead, the specific volume of IRF and its distribution across different retinal layers might have varied effects on the extent of intraretinal damage. In parallel, a larger serous PED or an increased volume of SRF could elevate the risk of involving the fovea, potentially leading to central vision loss.

These considerations highlight the prognostic need for detailed research into how the quantity of fluid in these distinct compartments—IRF, SRF, and sub-RPE fluid—differentially affects visual prognosis.

To fill this gap, we designed a study that employs a deep-learning fluid segmentation strategy to accurately quantify fluid volumes in Type 3 MNV eyes. By correlating the extent of IRF, SRF, and sub-RPE fluid with short-term VA outcomes following the loading dose of anti-VEGF injections, we aim to elucidate the differential impact of fluid volumes on visual prognosis. Moreover, we intend to investigate the specific role that the distribution of IRF—whether in the inner or outer layers of the retina—plays in the progression of vision loss in Type 3 MNV. This approach aims to enhance our understanding of how the relative proportions of different fluid types, beyond just their presence, impact visual outcomes in patients with Type 3 MNV.

METHODS

The IRBs involved in this study were notified about this retrospective cohort study that adhered to the 1964 Helsinki declaration and its later amendments. Participating patients provided informed consent for the retrospective use of their data. Analysis of data was made between September 2023 and December 2023.

We identified patients diagnosed with AMD by reviewing the medical records of three medical retina practices: San Raffaele Scientific Institute (Milan, Italy), Città della Salute e della Scienza Hospital (Turin, Italy), and Oftalvist Clinic (Valencia, Spain). Eligibility criteria for inclusion in the study required: (1) diagnosis of exudative AMD confirmed by the presence of intraretinal or subretinal fluid on structural OCT; (2) presence of a treatment-naïve Type 3 MNV confirmed by OCT angiography (OCTA) or dye-based angiography, as previously described;[2,3] (3) treatment with a loading dose of three monthly intravitreal injections of anti-VEGF therapy; and (4) follow-up assessment with structural OCT performed 30 ± 5 days after the third anti-VEGF injection. Patients were excluded if they presented with (1) any evidence of type 1 or type 2 MNV; (2) previous history of exudation; (3) history of amblyopia; (4) any other retinal or optic nerve condition; and (5) vitreoretinal interface disease; 6) previous vitreoretinal surgery.

All patients underwent structural OCT scans using the spectral domain (SD) Heidelberg Spectralis HRA + OCT (Heidelberg Engineering, Heidelberg, Germany) both at baseline—visit immediately preceding starting anti-VEGF treatment—and at the follow-up visit, 30 ± 5 days post the third anti-VEGF injection. The scanning protocol entailed 19 horizontal B-scans spaced 240 nm apart, spanning an area of roughly 5.5 × 4.5 mm (20° x 15°) centered on the fovea. Only images with a signal strength of at least 25, as per the manufacturer's recommendation, were considered. Best-corrected VA (BCVA) was recorded at both time points using Snellen charts and subsequently converted into the logarithm of the minimal angle of resolution (LogMAR) for analysis.

• **QUALITATIVE OCT ANALYSIS:** To determine eligibility, two experienced and unbiased graders (A.B. and E.B.) independently evaluated the baseline structural OCT images. The same readers then assessed the included eyes for qualitative features without knowledge of the visual outcomes. In cases of disagreement, an experienced clinician (F.B.) made the final decision.

At baseline, OCT images were evaluated for the presence of IRF, SRF, and sub-RPE fluid. IRF was defined as hyporeflective cysts located in the neuroretina, between the outer boundary of the ILM and the inner boundary of the ELM, SRF as hyporeflective spaces located between

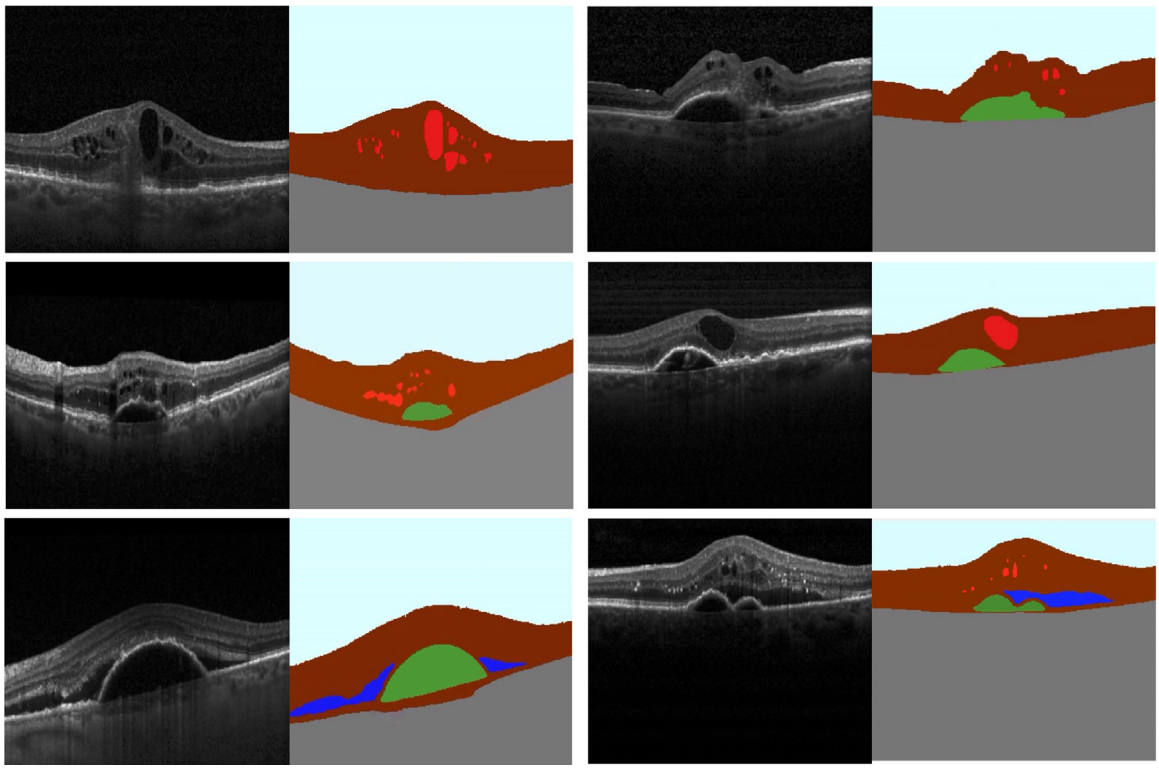

FIGURE 1. Example segmentation results of cases with treatment-naïve Type 3 MNV. Each row displays an OCT B-scan captured from a single patient. The left column exhibits the input OCT B-scans, the right column showcases the automated segmentation of vitreous, retina, choroid, and fluids. Notably, IRF is denoted in red, SRF in blue, sub-RPE fluid (serous PED) in green.

the outer boundary of the ELM and the inner boundary of the RPE, and sub-RPE fluid as serous PED, characterized by a dome-shaped, optically empty space between the RPE's outer boundary and Bruch's Membrane (BM) inner boundary. At baseline, the presence of complete RPE and outer retinal atrophy (cRORA) was also evaluated according to previously reported criteria.[19]

At the follow-up visit, the presence of signs of exudation (defined as IRF and SRF) and cRORA were graded.

• **QUANTITATIVE OCT ANALYSIS:** Baseline OCT B-scans were automatically segmented using the Orion software (Voxeleron Inc, Austin, USA) (Figure 1). The software performs layer segmentation as a preprocessing step to fluid segmentation. Retinal structure was automatically separated into the following individual layers: Retinal Nerve Fiber Layer (RNFL), Ganglion Cell-Inner Plexiform Layer (GCIPL), Inner Nuclear Layer (INL), Outer Plexiform Layer (OPL), Outer Nuclear Layer (ONL), subretinal space, and sub-RPE space. Following this, a validated deep learning algorithm processed each OCT B-scan, producing segmentation masks that identify and outline fluid regions, effectively distinguishing between IRF and SRF as well as sub-RPE fluid.[20,21] The accuracy of these fully automated outlines was manually validated by two independent graders (A.B. and E.B) by visual inspection of the algorithm's outlines and corresponding B-scans. Any OCT scan exhibiting segmentation errors was identified, and that eye was promptly excluded from further analysis to ensure the integrity of our data. The volumes of IRF, SRF, and sub-RPE fluid were then automatically computed by the software. IRF volume was calculated within the neuroretina (between the outer boundary of the ILM and the inner boundary of the ELM), the inner retina (between the outer boundary of the ILM and the outer boundary of the INL), and the outer retina (between the inner boundary of the OPL and the inner boundary of the ELM).

• **STATISTICAL ANALYSIS:** To assess for deviations from normal distribution, the Shapiro–Wilk test was applied to all variables. Mean values and standard deviations (SD) were calculated for each quantitative variable. Comparisons between visual acuities at baseline and follow-up were made using paired-sample T-tests. Comparisons between patients who resolved retinal fluids after exudation and those who did not were made using independent-sample T-tests.

Associations between baseline visual acuity, both qualitative and quantitative imaging factors, and final VA were investigated. Final VA, the primary outcome measure, was analyzed using a multiple regression analysis to identify significant predictors among the variables. Similarly, a

multiple regression analysis was conducted with baseline VA as the dependent variable to explore initial associations. Dependent factors included in the multiple regression analysis were those associated with a P-value $< .1$ in the univariable regression analysis.

All statistical analyses were carried out with the Jamovi software (version 2.4.12.0), setting the threshold for statistical significance at $P < .05$.

RESULTS

• BASELINE PATIENTS' CHARACTERISTICS AND LONGITUDINAL FUNCTIONAL AND MORPHOLOGICAL CHANGES: Two eyes had evidence of concomitant Type 1 MNV, one eye showed OCT evidence of an epiretinal membrane, and three eyes had images with a signal strength lower than 25. Additionally, four eyes were excluded due to fluid segmentation errors caused by artifacts in one or more B-scans, leading to over- or underestimation of fluids. A total of 46 eyes with treatment-naïve Type 3 MNV at baseline from 46 AMD patients were finally enrolled in this study. The mean ± SD age of participants was 82.3 ± 5.3 years (range 66-94 years), and 65.2% were women. All patients underwent a loading dose of 3 monthly anti-VEGF injections. Twenty-five eyes (54.3%) were treated with ranibizumab, 20 (43.5%) were treated with aflibercept, and 1 eye (2.2%) was treated with brolucizumab. At baseline assessment, 19 (41.3%) patients had bilateral MNV.

Visual acuity was 0.51 ± 0.30 LogMAR (Snellen equivalent of approximately 20/63) in the study eyes at baseline and 0.33 ± 0.20 LogMAR (Snellen equivalent of approximately 20/40) at the follow-up visit after the loading dose of anti-VEGF ($P < .001$). The mean distance between Type 3 MNV and fovea was 831.4 ± 362.2 μm.

At baseline, on structural OCT, IRF was graded to be present in 46 (100.0%) and 10 (21.7%) eyes at baseline and follow-up visits, respectively. Similarly, the presence of SRF was confirmed in 18 (39.1%) eyes at baseline and 0 (0.0%) eye at the follow-up visit after the loading dose of anti-VEGF. Sub-RPE fluid (i.e., visualized as serous PED as stated above) was instead diagnosed in 17 (36.9%) of patients at baseline and in 4 (8.7%) of patients at the follow-up visit. At baseline, out of the 18 eyes with sub-RPE fluid, 10 also had concomitant SRF. At baseline and follow-up, areas of cRORA were graded to be present in 3 (6.5%) and 31 (67.4%) eyes, respectively.

The IRF volume at baseline was 50.2 ± 71.1 nL and 121.6 ± 197.1 nL in the inner and outer retina, respectively. In the subgroup of patients with evidence of SRF, the SRF volume at baseline was 89.5 ± 93.5 nL. There was no statistically significant difference in the amount of IRF between patients with and without SRF ($P = 1.0$). In eyes exhibiting sub-RPE fluid at baseline, its volume was 570.8 ± 408.3 nL.

• COMPARISON OF VISUAL ACUITY BETWEEN PATIENTS WITH AND WITHOUT RESIDUAL FLUID AT THE FOLLOW-UP VISIT: After the loading dose of anti-VEGF therapy, 10 patients still exhibited evidence of fluid on structural OCT (i.e., all these patients had IRF, while none had SRF), whereas 36 eyes showed no signs of exudation. Visual acuity at the follow-up visit was 0.40 ± 0.17 LogMAR (approximately 20/50 Snellen equivalent) in patients with retinal fluid and 0.31 ± 0.20 LogMAR (approximately 20/40 Snellen equivalent) in eyes without retinal fluid ($P = .225$).

• REGRESSION ANALYSIS BETWEEN VISUAL ACUITY AND OCT FEATURES: Factors associated with visual acuities at baseline and follow-up visits are shown in Table 1. This analysis considered only patients exhibiting a complete resolution of retinal fluids after the loading dose ($n = 36$) to avoid the confounding effect of persistent retinal fluids.

Regarding baseline visual acuity, in the univariable analysis, both the presence of SRF, the distance of the MNV from the fovea, and the IRF volume in the inner retina were significantly associated with visual acuity. However, in the multivariable model, only the IRF volume in the inner retina ($P = .032$) and the distance of the MNV from the fovea ($P = .037$) remained significant predictors of visual acuity at baseline.

The follow-up VA was found to be associated with IRF in the inner retina ($P = .023$), while no significant associations were found between baseline outer retinal IRF volume and sub-RPE fluid volume with follow-up VA.

DISCUSSION

In this study, we employed a deep learning approach to detect and quantify retinal fluid in individuals with treatment-naïve AMD-associated exudative Type 3 MNV. These patients received a loading dose of intravitreal anti-VEGF therapy and were observed shortly thereafter upon achieving complete resolution of exudation.[22] Notably, the results of the present study demonstrated a significant relationship between the amount of IRF in the inner retina at baseline and short-term visual outcomes. Among the other OCT variables assessed at baseline, the amount of IRF in the outer retina, the presence of SRF, the presence of SHRM, and the SRF and sub-RPE fluid volumes did not significantly impact short-term visual outcomes. Since the purpose of our study was to investigate the associations between short-term visual outcomes and retinal fluids detected using OCT at baseline, in the analysis exploring associations between biomarkers and visual acuity, we did not include patients not resolving exudation after the loading dose of anti-VEGF therapy, as this could potentially affect visual

TABLE 1. Results of Univariable and Multivariable Analysis at the Baseline and Follow-Up Visits

	Univariable Analysis		Multivariable Analysis	
	Standardized Estimate (95% CI)	*P* Value	Standardized Estimate (95% CI)	*P* Value
Baseline visual acuity				
SRF at baseline visit: Y/N	0.280 (-0.055, 0.614)	.098#	0.270 (-0.047, 0.587)	.092
SHRM at baseline visit: Y/N	0.088 (-0.259, 0.435)	.610	-	-
IR-IRF volume at baseline visit	0.357 (0.031, 0.683)	.033#	0.349 (0.033, 0.666)	.032#
OR-IRF volume at baseline visit	0.175 (-0.168, 0.518)	.308	-	-
SRF volume at baseline visit	-0.208 (-0.549, 0.133)	.223	-	-
Sub-RPE fluid volume at baseline visit	0.040 (-0.308, 0.388)	.818	-	-
Distance between fovea and MNV	-0.319 (-0.649, 0.012)	.058#	-0.340 (-0.658, -0.022)	.037
Follow-up visual acuity				
SRF at baseline visit: Y/N	0.229 (-0.110, 0.569)	.179	-	-
SHRM at baseline visit: Y/N	0.0832 (-0.264, 0.431)	.629	-	-
IR-IRF volume at baseline visit	0.378 (0.056, 0.701)	.023#	0.378 (0.056, 0.701)	.023#
OR-IRF volume at baseline visit	0.216 (-0.125, 0.556)	.207	-	-
SRF volume at baseline visit	0.109 (-0.237, 0.456)	.525	-	-
Sub-RPE fluid volume at baseline visit	0.151 (-0.194, 0.495)	.380	-	-
Distance between fovea and MNV	-0.242 (-0.580, 0.096)	.155		

Significative P values are marked with #.

CI: confidence interval; **SRF:** subretinal fluid; **SHRM:** subretinal hyperreflective material; **IR:** inner retina; **OR:** outer retina; **IRF:** intraretinal fluid; **SRF:** subretinal fluid; **RPE:** retinal pigment epithelium; **MNV:** macular neovascularization.

acuity and introduce confounding variables into the results. More significantly, given the common occurrence of macular complications such as atrophy[23] and fibrosis[22] in eyes with Type 3 MNV, which can substantially impact long-term visual outcomes,[14] we felt the safer strategy was to focus on short-term outcomes where these complications are less prominent.

In neovascular AMD, the presence of intraretinal accumulation of fluid results from leakage into the neurosensory retina from the MNV.[17,24-26] Clinically, IRF remains the most critical predictive factor for both baseline visual acuity and subsequent visual acuity outcomes during treatment.[17,24-26] Ancillary quantitative studies have indicated that as much as 60% of the observed visual acuity in eyes with treatment-naïve neovascular AMD may be accounted for by the presence of IRF within the neurosensory layers.[27] Given that Type 3 MNV typically develops, grows, and exudates predominantly within the retina, the majority of cases with this type of neovascularization are distinguished by the existence of IRF.[28] This assumption is supported by the OCT staging system of Type 3 MNV proposed by Su et al.,[9] wherein all three stages of the exudative neovascularization are distinguished by the presence of IRF. Accordingly, all our patients with Type 3 MNV exhibit IRF at the initial assessment. Consequently, in Type 3 MNV, the sole presence of IRF may not be regarded as a reliable predictor, given its high prevalence among the studied population.

Chae et al.[16] previously attempted to quantify fluid in Type 3 MNV by measuring on OCT B-scans the height of intraretinal cysts, SRF, and PEDs. Their study aimed to establish correlations between these measurements and VA after a 1-year follow-up period. Differently from us, they found no significant relationship between these quantitative variables and visual outcomes. However, their methodology provided only an approximation of fluid volumes and failed to accurately quantify the total fluid present.

We added to the existing literature by also conducting a topographical analysis of IRF in patients with treatment-naïve Type 3 MNV. Specifically, this quantification involved categorizing the fluid based on the layer in which this was situated, resulting in volumes of IRF in the inner and outer retina, respectively. Crucially, the assessment of retinal fluids was conducted utilizing a deep learning methodology that has been previously validated, thus eliminating any potential for grading bias.

Importantly, the present study highlights the distinctive relationship between the amount of IRF and visual acuity in Type 3 MNV eyes: considering baseline and short-term visual acuity as the dependent variable, we observed a direct relationship with IRF volume in the inner retina, even after accounting for other anatomic factors, such as the presence of SHRM, volume of SRF, and sub-RPE fluid. Therefore, this analysis demonstrated that the volume of fluid in the inner retina at baseline was correlated with poorer baseline and short-term visual outcomes following the complete resolution of exudation subsequent to anti-VEGF therapy. In a previous study on eyes with diabetic macular edema, Tsuboi and colleagues[29] demonstrated that the fluid volume in the

inner retina emerged as the sole significant factor associated with visual acuity following treatment in a multivariable analysis. Hence, it could be suggested that the presence of fluid in the inner retina might damage pathways responsible for transmitting visual information from the photoreceptor to the ganglion cells.

The presence of SRF is also associated with exudation in neovascular AMD eyes.[28] Although SRF is usually associated with a more favorable visual prognosis in neovascular AMD, this OCT biomarker has been demonstrated to correlate with poorer visual acuity in Type 3 MNV cases.[17] Sharma and colleagues[17] conducted a retrospective analysis involving 56 eyes of 49 patients with treatment-naïve Type 3 MNV. In their study, IRF alone was observed in 31 (55.3%) eyes at baseline, while IRF was present alongside other compartmental fluids (i.e., SRF and/or sub-RPE fluid) in 23 eyes. The authors assessed visual outcomes following the complete resolution of fluid, regardless of the timing of resolution, with a follow-up period of 36.2 ± 29.1 months. They found that the final visual acuity differed between patients with only IRF at baseline compared to those with associated localization of fluid in other compartments, with final BCVA that was worse in the latter patients. However, the latter study had limitations in assessing the impact of IRF on visual acuity, as it did not offer quantitative data on IRF.[18] As mentioned earlier, a quantitative evaluation of this fluid may be crucial for Type 3 MNV, given that all patients with this type of neovascularization exhibit intraretinal localization of fluid. In our study, after conducting multivariable analysis, we found that neither the presence nor the quantity of SRF was correlated with baseline or follow-up visual acuities.

Our study has limitations that should be considered when interpreting our results. The primary limitation is the relatively small sample size. Additionally, the retrospective study design further restricts the generalizability of our findings. Furthermore, a denser raster scan would have provided more precise fluid quantification. Despite this, the 19 horizontal B-scan protocol we used effectively covers the entire macula and offers an overview of the relative proportions of fluid in different compartments.

However, our study also has strengths. Importantly, we employed a deep learning algorithm to segment fluids, which minimizes susceptibility to inter-reader variability.

In summary, the present study showed that eyes with Type 3 MNV are commonly complicated by IRF at baseline. Consequently, in such cases, quantifying the volume of fluid within retinal layers may hold prognostic significance, as our results suggest a potential correlation between the amount of fluid in the inner retina and visual outcomes. This observation aligns with speculation in other disorders where inner retinal fluid presence may disrupt connections between photoreceptors and ganglion cells, possibly leading to visual impairment.[29] Future prospective studies with extended follow-up periods could validate our findings and ascertain whether the quantity of retinal fluid in the inner retina might serve as a biomarker for long-term visual outcomes, complementing its role in short-term visual prognostication.

CREDIT AUTHORSHIP CONTRIBUTION STATEMENT

ALESSANDRO BERNI: Writing – review & editing, Writing – original draft, Validation, Methodology, Formal analysis, Data curation, Conceptualization. **JONATHAN D. OAKLEY:** Software, Methodology, Formal analysis. **ROSA DOLZ-MARCO:** Writing – review & editing, Formal analysis. **ROBERTO GALLEGO-PINAZO:** Writing – review & editing, Validation, Formal analysis. **FRANCESCA CIMOROSI:** Writing – review & editing, Formal analysis, Data curation. **ANDREA GHILARDI:** Writing – review & editing, Formal analysis, Data curation. **DANIEL B. RUSSAKOFF:** Writing – review & editing, Methodology, Formal analysis. **COSTANZA BARRESI:** Writing – review & editing, Formal analysis, Data curation. **UGO INTROINI:** Writing – review & editing, Formal analysis, Data curation. **MICHELE REIBALDI:** Writing – review & editing, Validation, Supervision, Methodology, Investigation, Funding acquisition, Formal analysis, Data curation, Conceptualization. **FRANCESCO BANDELLO:** Writing – review & editing, Supervision, Resources, Methodology, Funding acquisition, Formal analysis, Data curation, Conceptualization. **ENRICO BORRELLI:** Writing – review & editing, Writing – original draft, Supervision, Methodology, Formal analysis, Data curation, Conceptualization.

Funding/Support: None. Financial Disclosures: Jonathan D. Oakley: Employees (Voxeleron Inc, Austin, USA), Patent (Voxeleron Inc, Austin, USA); Daniel B. Russakoff: Employees (Voxeleron Inc, Austin, USA), Patent (Voxeleron Inc, Austin, USA); Rosa Dolz-Marco is a consultant for: Alexion, Apellis, Heidelberg Engineering, Hofmann La Roche; Roberto Gallego-Pinazo is a consultant for: Alexion, Apellis, Boehringer Ingelheim, ORA Clinical, Hofmann La Roche, Zeiss; Michele Reibaldi is a consultant for: Abbvie, Bayer, Roche, Novartis; Francesco Bandello is a consultant for: Abbvie, Alimera, Bayer, Boehringer-Ingelheim, Fidia Sooft, Hofmann La Roche, Novartis, Ntc Pharma, Oxurion Nv, Sifi. Enrico Borrelli is a consultant for: Abbvie, Bayer, Hofmann La Roche, Zeiss. Other authors: None. Author Contributions: Study concept and design: Berni A, Reibaldi M, Bandello F, and Borrelli E. Acquisition, analysis, or interpretation of data: All authors. Drafting of the manuscript: Berni A and Borrelli E. Critical revision of the manuscript for important intellectual content: All authors. Statistical analysis: Berni A and Borrelli E. Study supervision: Berni A, Reibaldi M, Bandello F, and Borrelli E.

REFERENCES

1. Yannuzzi LA, Negrao S, Iida T, et al. Retinal angiomatous proliferation in age-related macular degeneration. *Retina*. 2001;21(5):416–434. doi:10.1097/00006982-200110000-00003.
2. Freund KB, Ho IV, Barbazetto IA, et al. Type 3 neovascularization: the expanded spectrum of retinal angiomatous proliferation. *Retina*. 2008;28(2):201–211. doi:10.1097/IAE.0b013e3181669504.
3. Freund KB, Zweifel SA, Engelbert M. Do we need a new classification for choroidal neovascularization in age-related macular degeneration? *Retina*. 2010;30(9):1333–1349. doi:10.1097/IAE.0b013e3181e7976b.
4. Grossniklaus HE, Gass JD. Clinicopathologic correlations of surgically excised Type 1 and Type 2 submacular choroidal neovascular membranes. *Am J Ophthalmol*. 1998;126(1):59–69. doi:10.1016/s0002-9394(98)00145-7.
5. Borrelli E, Mastropasqua L, Souied E, et al. Longitudinal assessment of Type 3 macular neovascularization using 3D volume-rendering OCTA. *Can J Ophthalmol*. 2022;57(4):228–235. doi:10.1016/j.jcjo.2021.04.020.
6. Jung JJ, Chen CY, Mrejen S, et al. The incidence of neovascular subtypes in newly diagnosed neovascular age-related macular degeneration. *Am J Ophthalmol*. 2014;158(4):769–779.e2. doi:10.1016/j.ajo.2014.07.006.
7. Nagiel A, Sarraf D, Sadda SR, et al. Type 3 neovascularization: evolution, association with pigment epithelial detachment, and treatment response as revealed by spectral domain optical coherence tomography. *Retina*. 2015;35(4):638–647. doi:10.1097/IAE.0000000000000488.
8. Chen X, Al-Sheikh M, Chan CK, et al. Type 1 versus type 3 neovascularization in pigment epithelial detachments associated with age-related macular degeneration after anti-vascular endothelial growth factor therapy: a prospective study. *Retina*. 2016;36(suppl 1):S50–S64. doi:10.1097/IAE.0000000000001271.
9. Su D, Lin S, Phasukkijwatana N, et al. An updated staging system of Type 3 neovascularization using spectral domain optical coherence tomography. *Retina*. 2016;36(suppl 1):S40–S49. doi:10.1097/IAE.0000000000001268.
10. Miere A, Querques G, Semoun O, et al. Optical coherence tomography angiography changes in early Type 3 neovascularization after anti-vascular endothelial growth factor treatment. *Retina*. 2017;37(10):1873–1879. doi:10.1097/IAE.0000000000001447.
11. Phasukkijwatana N, Tan ACS, Chen X, Freund KB, Sarraf D. Optical coherence tomography angiography of Type 3 neovascularisation in age-related macular degeneration after antiangiogenic therapy. *Br J Ophthalmol*. 2017;101(5):597–602. doi:10.1136/bjophthalmol-2016-308815.
12. Grunwald JE, Daniel E, Huang J, et al. Risk of geographic atrophy in the comparison of age-related macular degeneration treatments trials. *Ophthalmology*. 2014;121(1):150–161. doi:10.1016/j.ophtha.2013.08.015.
13. Domalpally A, Danis RP, Trane R, et al. Atrophy in neovascular age-related macular degeneration: age-related eye disease study 2 report number 15. *Ophthalmol Retina*. 2018;2(10):1021–1027. doi:10.1016/j.oret.2018.04.009.
14. Barresi C, Borrelli E, Fantaguzzi F, et al. Complications associated with worse visual outcomes in patients with exudative neovascular age-related macular degeneration. *Ophthalmologica*. 2021;244(6):512–522. doi:10.1159/000519518.
15. Borrelli E, Barresi C, Ricardi F, et al. Distinct pathways of macular atrophy in Type 3 macular neovascularization associated with AMD. *Investigat Ophthalmol Vis Sci*. 2024;65(3):18. doi:10.1167/iovs.65.3.18.
16. Chae B, Su D, Gal-Or O, Freund KB, Sarraf D. Type 3 neovascularisation: long-term analysis of visual acuity and optical coherence tomography anatomical outcomes. *Br J Ophthalmol*. 2019;103(1):43–48. doi:10.1136/bjophthalmol-2018-311850.
17. Sharma A, Cheung CMG, Arias-Barquet L, et al. Fluid-based visual prognostication in Type 3 macular neovascularization-flip-3 study. *Retina*. 2022;42(1):107–113. doi:10.1097/IAE.0000000000003261.
18. Haj Najeeb B, Deak GG, Gerendas BS, Schmidt-Erfurth U. Correspondence. *Retina*. 2022;42(1):e10–e11. doi:10.1097/IAE.0000000000003355.
19. Sadda SR, Guymer R, Holz FG, et al. Consensus definition for atrophy associated with age-related macular degeneration on OCT: classification of atrophy report 3. *Ophthalmology*. 2018;125(4):537–548. doi:10.1016/j.ophtha.2017.09.028.
20. Borrelli E, Oakley JD, Iaccarino G, et al. Deep-learning based automated quantification of critical optical coherence tomography features in neovascular age-related macular degeneration. *Eye (Lond)*. 2024;38(3):537–544. doi:10.1038/s41433-023-02720-8.
21. Ricardi F, Oakley J, Russakoff D, et al. Validation of a deep learning model for automatic detection and quantification of five OCT critical retinal features associated with neovascular age-related macular degeneration. *Br J Ophthalmol*. 2024. doi:10.1136/bjo-2023-324647.
22. Forte P, Fontana V, Muzio J, et al. Predictors of 24-month onset of macular fibrosis in Type 3 macular neovascularisation. *Br J Ophthalmol*. 2024. doi:10.1136/bjo-2023-324713.
23. Staurenghi G, Cozzi M, Sadda S, Hill L, Gune S. Characteristics that correlate with macular atrophy in ranibizumab-treated patients with neovascular age-related macular degeneration. *Ophthalmol Retina*. 2023;7(4):300–306. doi:10.1016/j.oret.2022.11.002.
24. Schmidt-Erfurth U, Waldstein SM. A paradigm shift in imaging biomarkers in neovascular age-related macular degeneration. *Prog Retin Eye Res*. 2016;50:1–24. doi:10.1016/j.preteyeres.2015.07.007.
25. Jaffe GJ, Ying GS, Toth CA, et al. Macular morphology and visual acuity in year five of the comparison of age-related macular degeneration treatments trials. *Ophthalmology*. 2019;126(2):252–260. doi:10.1016/j.ophtha.2018.08.035.
26. Kaiser PK, Wykoff CC, Singh RP, et al. Retinal fluid and thickness as measures of disease activity in neovascular age-related macular degeneration. *Retina*. 2021;41(8):1579–1586. doi:10.1097/IAE.0000000000003194.
27. Borrelli E, Vigano C, Battista M, et al. Individual vs. combined imaging modalities for diagnosing neovascular central serous chorioretinopathy. *Graefes Arch Clin Exp Ophthalmol*. 2023;261(5):1267–1273. doi:10.1007/s00417-022-05924-y.

28. Najeeb BH, Gerendas BS, Deak GG, Leingang O, Bogunovic H, Schmidt-Erfurth U. An automated comparative analysis of the exudative biomarkers in neovascular age-related macular degeneration, the RAP study: report 6. *Am J Ophthalmol*. 2024;264:53–65. doi:10.1016/j.ajo.2024.02.018.

29. Tsuboi K, You QS, Guo Y, et al. Association between fluid volume in inner nuclear layer and visual acuity in diabetic macular edema. *Am J Ophthalmol*. 2022;237:164–172. doi:10.1016/j.ajo.2021.12.012.